International Journal of Heat and Mass Transfer 127 (2018) 751–767

Contents lists available at ScienceDirect

International Journal of Heat and Mass Transfer

journal homepage: www.elsevier.com/locate/ijhmt

Heat transfer enhancement on a surface of impinging jet by increasing entrainment using air-augmented duct

C. Nuntadusit *, M. Wae-hayee, N. Kaewchoothong

Department of Mechanical Engineering, Faculty of Engineering, Prince of Songkla University, Thailand

ARTICLE INFO

Article history:
Received 23 March 2018
Received in revised form 27 June 2018
Accepted 27 June 2018

Keywords:
Impinging jet
Air-augmented duct
Air entrainment
Heat transfer enhancement
Thermal infrared camera
Hot-wire anemometer
CFD

ABSTRACT

Flow and heat transfer characteristics of impinging jet from pipe nozzle with air-augmented duct were experimentally and numerically investigated. The effects of air-augmented duct geometry on heat transfer enhancement were concerned. The experimental parameters included a diameter (D) and a length (L) of air-augmented duct in the range of $D = 2d$, $3.3d$, $6d$, and $L = 2d$, $4d$, $6d$ where d was the inner diameter of main pipe nozzle at 17.2 mm. The distance from air-augmented duct outlet to impingement surface (S) at $S = 2d$, $4d$ and $6d$ were considered. The conventional impinging jet was also studied to compare the results with the case of an air-augmented duct. The result comparison was based on constant jet mass flow rate by fixing the jet Reynolds number of conventional pipe at $Re = 20{,}000$. The temperature distributions on the impingement surface were measured by using a thermal infrared camera, and profiles of velocity and turbulence intensity of the jet were measured by using hot-wire anemometer. The 3-D numerical simulation with SST k-ω turbulence model was also applied to reveal the flow characteristics. The results show that the heat transfer rate on the impingement surface for the case of an air-augmented duct in conditions of $2d \leq D \leq 4d$ and $L = 2d$ is noticeably higher than the case of conventional impinging jets due to increasing air entrainment. The heat transfer rate for the case of $D = 6d$, $L = 2d$ at $S = 2d$, is the largest by getting 25.42% higher compared to a conventional impinging jet.

1. Introduction

Turbulent impinging jets are widely employed in thermal industrial applications such as tempering of glass, drying of paper, cooling of electronics and turbine engine components due to high heat transfer on stagnation regions. Previous works have extensively studied flow and heat transfer characteristics of impinging jets. Heat transfer rates on impingement surfaces are governed by momentum of jet impingements on target surfaces and turbulence intensity of jets just before impingement. Generally, after jet discharging from a nozzle, the spreading jet results in the reducing of axial velocity and the increasing of turbulence intensity in a jet flow. The optimal matching between axial velocity and turbulence intensity can be found at the end of a potential core occurring in the range of 5–8 times nozzle diameter from jet outlet, depending on nozzle shape and jet Reynolds number. Subsequently, the maximum heat transfer at stagnation region is achieved [1–5].

Many researchers have devoted their studies to enhancing heat transfer on an impingement surface by increasing turbulence intensity of jet flow. Popular methods to accomplish this are attaching mesh screens [6] or triangular tabs at the jet outlet [7] and inserting twisted tape into pipe nozzle [8–11] or guide vanes into pipe nozzle [12,13]. So, an important factor to enhance turbulence intensity of jet flow is to increase entrainment of ambient fluid.

Expanding a jet outlet is a simple method to increase the entrainment of ambient fluid into the jet flow [14–19]. Generally, this method is adopted to increase the mixing and spreading of a jet in combustion of industrial applications [20,21]. However, it may yet be adopted for enhancing heat transfer on an impingement region.

In this work, an impinging jet associated with a short pipe called an "air-augmented duct" is employed to increase heat transfer on impingement surfaces. Ambient air would be increasingly sucked through air-augmented duct for enhancing turbulent intensity into a jet flow. Hence, the geometry of air-augmented duct must be explored to gain an optimum heat transfer on an impingement surface.

The aim of this study is to investigate flow and heat transfer characteristics of an impinging jet from pipe nozzle with air-augmented duct experimentally and numerically. The length and diameter of air-augmented duct as well as the distance from air-augmented duct outlet to impingement surface were

* Corresponding author.
E-mail address: chayut.n@psu.ac.th (C. Nuntadusit).

https://doi.org/10.1016/j.ijheatmasstransfer.2018.06.130
0017-9310/

Nomenclature

A	area of heat transfer surface
d	diameter of pipe nozzle
D	diameter of air-augmented duct
h	heat transfer coefficient
$h_{loss,nc}$	heat transfer coefficient for loss by natural convection
H	pipe nozzle outlet-to-impingement surface distance
I	electrical current
k	thermal conductivity
L	length of air-augmented duct
L_w	length of heat transfer surface
Nu	Nusselt number
$\overline{Nu}$	area-averaged Nusselt number
$\dot{q}_{input}$	heat flux input
$\dot{q}_{loss,rad}$	heat loss due to radiation
$\dot{q}_{loss,nc}$	heat loss due to natural convection
Re	Reynolds number of jet
S	distance from air-augmented duct outlet to impingement surface
T_{aw}	local adiabatic wall temperature
T_j	jet temperature
T_w	local wall temperature
$\overline{T_w}$	average wall temperature
T_s	surrounding temperature
TKE	turbulent kinetic energy
u'	fluctuation velocity on X-axis direction
V	electrical voltage in Eq. (2), average velocity
V_0	average velocity at the center of jet outlet
v'	fluctuation velocity on Y-axis direction
W	average velocity on jet axial direction
W_0	average velocity on jet axial direction at the center of jet outlet
W_w	width of heat transfer surface
w'	fluctuation velocity on jet axial direction
X, Y, Z	Cartesian coordinate components
Z^*	coordinate in Z-axis direction started from air-augmented duct outlet
Greek symbols	
ε	emissive coefficient
σ	Stefan-Boltzmann constant

examined. The results were compared to a conventional impinging jet under the same mass flow rate. The heat transfer characteristics on the impingement surface were detected using an infrared camera, and the flow characteristics of the impinging jet were determined by hot-wire anemometer and numerical simulation using ANSYS Ver.13.0 (Fluent).

2. Experimental setup and method

2.1. Study models and parameters

The models of the impinging jet from conventional pipe nozzle and nozzle with air-augmented duct are shown in Fig. 1. The jet was discharged from a nozzle pipe and perpendicularly impinged on a flat surface. The concentric air-augmented duct was assembled at the end of the pipe nozzle as shown in Fig. 1(b). An origin of the Cartesian coordinates was located at the center of the jet exit. The *Z*-axis is on the axial of jet; *X*-axis and *Y*-axis are normal to the axial of jet in horizontal and vertical directions, respectively. Z^*-axis is also defined on the axial of jet started at exit of air-augmented duct.

The inner diameter of the main pipe nozzle (d) was 17.2 mm. The length (L) and inner diameter (D) of air-augmented duct were varied at $L = 2d$, $4d$ and $6d$, and $D = 2d$, $3.3d$, $4d$, $6d$ and $8d$, respectively. In addition, the distance from the air-augmented duct outlet to impingement surface (S) was varied at $S = 2d$, $4d$ and $6d$. The conventional pipe nozzle was also studied to benchmark the results with the case of air-augmented duct. It should be noted that the jet-to-surface distance (H, distance from pipe nozzle outlet to impingement surface) was varied at $H = 2d$, $4d$, $6d$, $8d$, $10d$ and $12d$ in relation to the proportional variation of the air-augmented duct length (L) and the distance from the air-augmented duct outlet to impingement surface (S). The comparisons were based on a constant jet mass flow rate by fixing the jet Reynolds number of the conventional impinging jet at $Re = 20{,}000$ (calculated from velocity at the center of pipe exit).

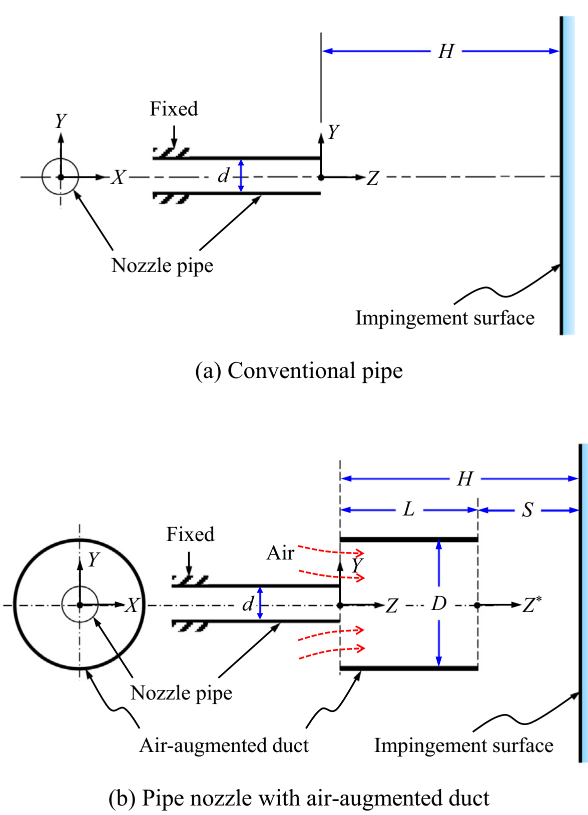

Fig. 1. Detail of study models.

2.2. Experimental setup

The diagram of experimental setup is shown in Fig. 2. The 1-HP blower accelerated the air which flowed through the orifice flow meter and temperature controlled chamber equipped with a 2-kW heater. The temperature of the air jet was controlled with a temperature controller and a power controller at 27.0 ± 0.2 °C. The flow rate of the air jet was controlled by adjusting the rotating speed of blower with an inverter. The turbulent jet discharged from the round pipe with inner diameter of $d = 17.2$ mm and length to diameter ratio of 83. This pipe length was long enough to ensure the flow being fully developed at the pipe exit. Two